Influence of substrate on the electrodeposition of nickel-molybdenum alloys

J. CROUSIER, M. EYRAUD, J.-P. CROUSIER

Laboratoire de Physico-Chimie des Matériaux, équipe Corrosion et Electrochimie. Université de Provence, 13331 Marseille, Cedex 3, France

J.-M. ROMAN

Société Neyrpic, 38041 Grenoble, Cedex, France

The electrodeposition of nickel-molybdenum alloy has been studied on various substrates with the aim of determining the influence of hydrogen evolution on the formation of the deposit. Transient electrochemical methods were used. Three types of substrates were used. Glassy carbon in which hydrogen absorption cannot occur, palladium in which hydrogen diffusion is rapid, and nickel. Good and thick deposits were obtained on glassy carbon and annealed ultra pure nickel. On palladium no deposit was formed. The importance of hydrogen in the formation of the deposit was confirmed. Codeposition occurs in the same potential range as hydrogen evolution, and therefore hydrogen is trapped in the expanding lattice as seen by its oxidation during anodic polarization.

1. Introduction

Nickel-molybdenum alloys are very interesting as coatings for corrosion protection because their composition corresponds to Hastelloys which are well known for their good corrosion resistance. They also offer good catalytic properties for hydrogen evolution in alkaline solutions, showing substantial depolarization in comparison with the iron group metals [1-3]. Molybdenum has never been deposited in the metallic state, though one investigation [4] has established the reduction of molybdate in an adherent brown molybdenum oxide and further reduction of this oxide by hydrogen. This result is probably associated with the presence of metallic iron group impurities, which make possible the deposition of molybdenum–iron group alloys. Therefore the deposition of NiMo is typically and induced codeposition.

Molybdenum has been codeposited with metals such as Ni, Fe and Co, mainly from citrate solutions, which make it possible to obtain good quality and rich molybdenum alloys, plated by pulsed or continuous currents [5-7]. Rich molybdenum alloys have also been deposited, at high current density, from pyrophosphate baths [8]. All the authors agree with a mechanism in two steps with the formation of a molybdenum-nickel oxide, further reduced by hydrogen to a metallic molybdenum–nickel alloy.

Recent work on this topic was performed by Chassaing and Vu Quang [7] using impedance measurement. They propose a two step mechanism: First the formation of a MoO_2 oxide which, in the presence of Ni^{2+}, gives a mixed oxide MoO_2Ni_4
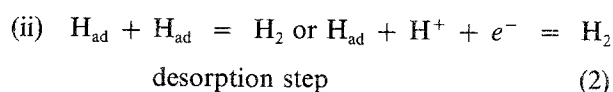
$$MoO_2 + 4Ni^{2+} + 8e^- = MoO_2Ni_4$$
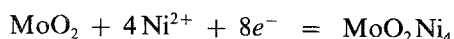
and then the reduction of this oxide by hydrogen to form $MoNi_3$ with included hydrogen, thus

$$MoO_4^{2-} + 3Ni^{2+} + 8e^- + (4 + n)H \rightarrow MoNi_3$$
$$+ 4OH^- + nH_{included}$$
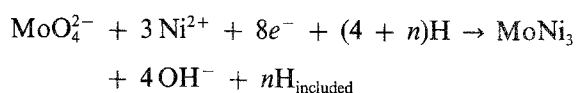
The deposit so obtained was poorly crystallized.

The role of hydrogen is recognized in all studies devoted to this alloy, i.e. hydrogen evolution being strongly dependent on the chemical nature of the cathode–metal. The aim of the present work was to investigate the mechanism of the nickel-molybdenum deposition onto various substrates.

The hydrogen evolution on a metal occurs in two main steps:

(i) $\quad H^+ + e^- = H_{ad} \quad$ discharge step $\qquad$ (1)

(ii) $\quad H_{ad} + H_{ad} = H_2$ or $H_{ad} + H^+ + e^- = H_2$

$\qquad$ desorption step $\qquad\qquad\qquad\quad$ (2)

Sometimes, a third step is involved [9]

(iii) $\quad H_{ad} \rightarrow H_{included} \qquad\qquad\qquad\qquad$ (3)

The substrates used were selected according to their known behaviour for hydrogen evolution in sulphuric acid solution, assuming that in citric acid solution the behaviour is similar, and hence the experiments were performed on three substrates: two substrates with opposite behaviour towards hydrogen evolution (vitreous carbon on which Reaction 3 cannot occur, palladium into which hydrogen diffusion is rapid), and one substrate whose behaviour is between palladium and carbon (nickel in two purity states). On this latter substrate some heat treatment was performed to check the influence of the microstructure.
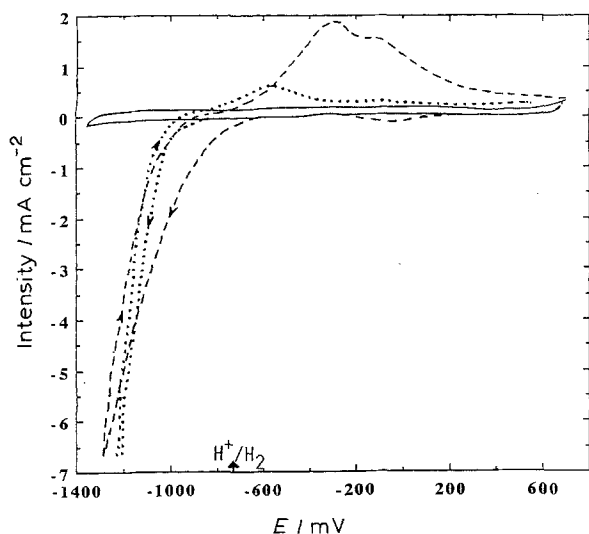
Fig. 1. Voltammograms from citrate solution without plating salts on: glassy carbon (——), 99.9% Ni (· · · ·), palladium (– – –). Scan rate 50 mV s^{-1}.

2. Experimental procedure

All the experiments were conducted in the following citrate solution from [7] at 25°C: $Na_2MoO_4 \cdot 2H_2O$, 0.015 M; $NiSO_4 \cdot 7H_2O$, 0.2 M; and $Na_3Cit \cdot 2H_2O$, 0.25 M. This is referred to as NiMo solution.

Solutions of the same composition but without molybdate (referred to as Ni solution), or without nickel sulphate (referred to as Mo solution) were used to compare the deposition of nickel, molybdenum and nickel-molybdenum.

The solutions were deaerated by argon bubbling and not stirred. A conventional three-electrode cell was used. The counter electrode was a large platinium sheet in order to avoid change in the metallic ion concentration of the solution. The working electrodes were: discs of vitreous carbon (area 0.07 cm^2), of 99.9% Ni, 99.999% Ni (area 1 cm^2), and palladium (area 0.2 cm^2), embedded in resin.

Before each experiment, the specimens were polished with emery paper, then with diamond powder on a polishing cloth, cleaned in an ultrasonic bath, and dipped in the solution without drying. All potentials were reported with respect to a saturated calomel electrode. The instrumentation for the experiments consisted of a PAR 273 potentiostat interfaced with an IBM computer. Transient methods were used: cyclic voltammetry, and galvanostatic and potentiostatic polarizations.

3. Results

3.1. Hydrogen evolution on different substrates

Figure 1 shows voltammograms for the various substrates in citrate solutions without the plating salts. They make it possible to classify the different substrates in the order: C > Ni > Pd, according to their hydrogen evolution overpotentials. On vitreous carbon there is no current down to − 1400 mV. An interesting feature is the large anodic peak on the
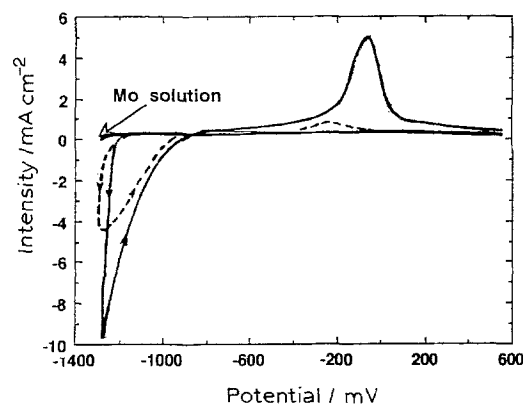

Fig. 2. Voltammograms from Mo solution, Ni solution (– – –), and Ni–Mo solution (——), on glassy carbon. Scan rate 50 mV s^{-1}.

reverse scan in the case of palladium. This peak could be the palladium dissolution peak, but actually this anodic peak is attributed to the oxidation of absorbed hydrogen [10]. The arrow in Fig. 1 indicates the value of the equilibrium potential of the H^+/H_2 couple. The anodic peak in the nickel voltammogram is also in the potential range of hydrogen oxidation.

3.2. Glassy carbon substrate

Figure 2 presents two voltammograms recorded for the carbon substrate from Ni solution and Ni–Mo solution. On the forward scan, no current is observed down to about − 1150 mV, where the cathodic current, for both the solutions, increases steeply. The scan is reversed at − 1300 mV, and the current intensity is higher on the reverse scan and reaches zero at − 720 mV for both Ni solution and Ni–Mo solution. The cathodic part of these curves has the characteristic steep increase in current and nucleation loop of metal deposition occuring by nucleation. On the reverse scan, the current increases slowly before the formation of an anodic peak. Although this peak looks like a stripping peak, it must be related to another oxidation reaction, as will be seen in the global study of the anodic part of the voltammograms.

The voltammogram, recorded in solution containing only molybdate, referred to as the Mo solution, shows neither a cathodic nor an anodic peak, proving that no electron transfer occurs over this potential range.

In a series of pulse experiments, the potential was stepped from an anodic potential, where no electrochemical reaction occurs, to a value determined on the corresponding voltammogram. Figure 3 presents a set of current-time transients from Ni solution and Fig. 4 a set of transients from the NiMo solution. They show an increase in current up to a maximum which is typical for the formation of a deposit by nucleation and growth of crystallites. The transients from Mo solution (Fig. 3) show monotonic decreases in current down to zero, again showing that no reaction occurs.

Figure 5 presents, for comparison, the current-time transients for Ni and NiMo solutions on the same time scale, for two potential steps. The beneficial effect of molybdenum addition to the Ni solution is confirmed, the increase in the maximum current is accompanied
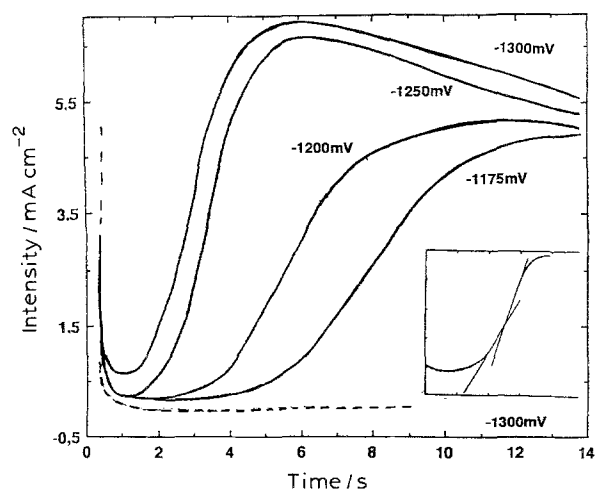
Fig. 3. Current–time transients from Mo solution (– – –), and Ni solution (——), on glassy carbon.

Fig. 5. Comparison between current–time transients from Ni solution and Mo–Ni solution on glassy carbon at (——) − 1300 and (– – –) − 1200 mV.

by a reduction of the induction period before the rising current which was observed in the case of the *Ni solution*.

The effect of stirring the solution was tested in the case of the *NiMo solution*. The voltammetry experiment shows an increase of the nucleation overpotential and this result is confirmed by the potential step experiments. Figure 6 shows the effect of stirring on the current-time transients recorded for the same step (− 1250 mV). The slope of the rising part decreases with stirring but the current maximum does not change what would happen if the deposition was diffusion controlled.

The early part of the rising transients, by plotting log i against log t, and determining the slope of the linear part (insert in Fig. 3) makes it possible to determine the kinetic control of nuclei growth. The value of the slope in the case of the *Ni solution* is 3, which indicates that the nickel deposit is formed by progressive nucleation followed by three dimensional growth under electron transfer control. This linear part is preceeded by a further linear part, of very short duration, whose slope is about 2, indicating instantaneous nucleation. This instantaneous nucleation, preceeding another mechanism, is not surprising and
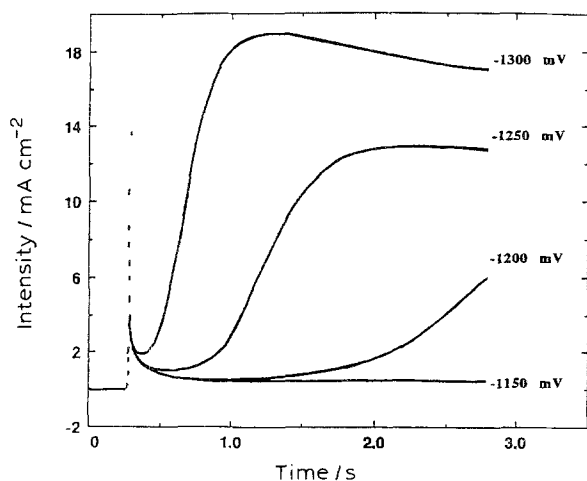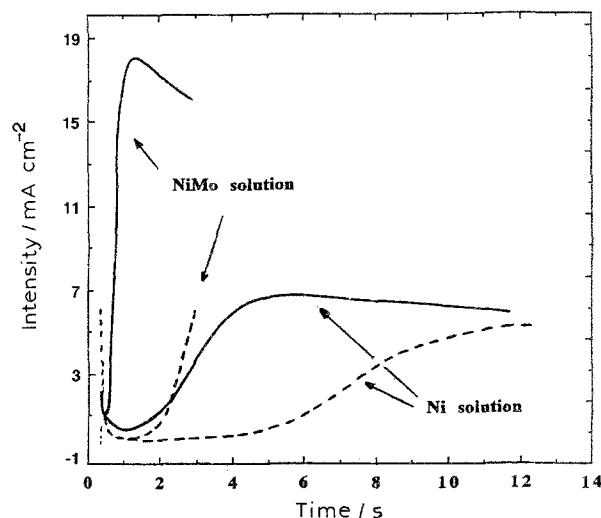
is probably associated with most of the deposits, but is often difficult to observe for fast nucleation processes. In the case of the *NiMo solution*, it is impossible to determine a slope corresponding to a known mechanism because of the codeposition.

Though current step experiments are often difficult to interpret, they can give valuable information. Figure 7 presents the potential-time transients obtained for − 140 μA and − 700 μA. A peak potential occurs for the highest current. The appearance of such a maximum in the galvanostatic transient has been related to a two-step process [11] and indicates that the applied current is greater than a critical value; this peak does not exist if the applied current is − 140 μA.

Bulk deposits were prepared on vitreous carbon by polarizing cathodically at − 1200 mV for 3 h. Two solutions of pH 7 and 10 were tested. In both cases the deposits were bright, smooth and peeled off. The deposits obtained for the same polarization time were thicker from the solution at pH 10 than from the solution at pH 7. X-ray diffraction studies of the deposits show a broad peak, and therefore it is concluded that they are poorly crystallized, if at all. Considering their smooth aspect, they are probably amorphous.
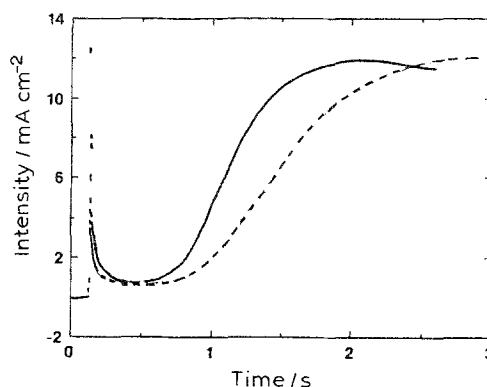

Fig. 4. Current–time transients from Ni–Mo solution on glassy carbon.

Fig. 6. Current–time transients (applied potential − 1250 mV) from Ni–Mo solution, (– – –) stirred and quiescent (——), on glassy carbon.
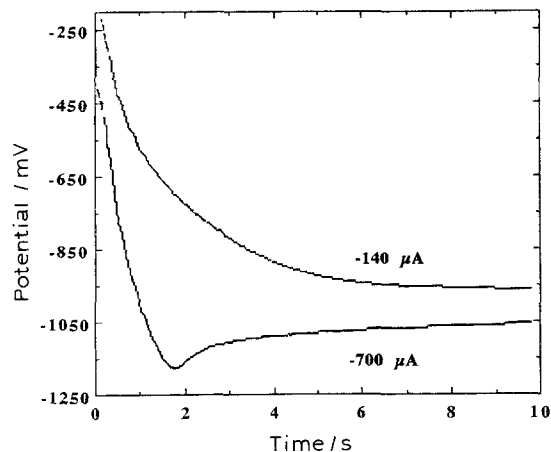
Fig. 7. Potential–time transients from Ni–Mo solution on glassy carbon.

3.3. *Nickel substrates*

Figure 8 presents the voltammograms obtained from the *Ni–Mo solution* on nickel substrates. For the 99.9% pure Ni and the 99.999% pure Ni, instead of a steep increase of the cathodic current, the current increases slowly. This voltammogram does not correspond to the formation of a deposit by a nucleation mechanism.

To check whether there is formation of a deposit, the 99.9% Ni electrode was polarized at $-1200 \, mV$ for 7 h. There is no formation of a bulk deposit, but the electrode surface was covered by a very thin bright film, without any bearing on the charge supplied, which peeled off and could result from the formation of a molybdenum oxide by reduction of sodium molybdate [12] or by a very thin Ni–Mo alloy.

Current step experiments were performed from citrate solution, *Mo solution, Ni solution* and *Ni–Mo solution* onto 99.9% Ni. Figure 9 presents the potential–time transients. The stabilized potentials for the experiments performed from *Ni* and *Ni–Mo solutions* are higher than for the two other solutions, showing that a surface change occurs. A set of current–time transients obtained from *Ni–Mo solution* on 99.9% Ni is presented in Fig. 10. These are difficult to interpret, nevertheless a maximum current occurs, provided the
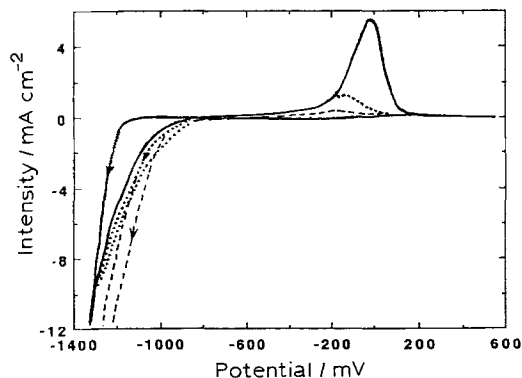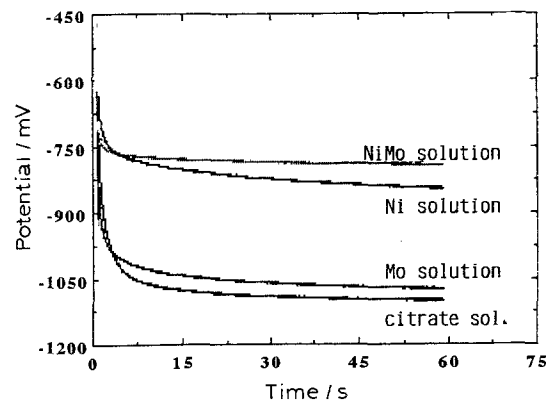

Fig. 9. Potential–time transients from citrate solution, Mo solution, Ni solution and Ni–Mo solution on 99.9% Ni substrate. ($i = -150 \, \mu A \, cm^{-2}$).

potential is more negative than $-1000 \, mV$, which may indicate the formation of a deposit.

The thick deposits obtained by Chassaing [7] from the same *Ni–Mo solution* as in the present work were crystallized onto high-purity nickel (less than 10 p.p.m. impurities), similar to the 99.999% Ni used in this work. To check if there is an effect of the metal structure, the commercial 99.999% Ni was carefully annealed (referred to as Nianneal) to form large grains. The grain size increase was checked, after etching, by microscopic examination. Then a new voltammogram was traced with the Nianneal electrode (Fig. 8). This presents the characteristic steep increase in cathodic current. The potential at zero current on the reverse trace has the same value as that recorded from the *Ni–Mo solution* onto glassy carbon. The anodic part shows one peak at the same potential as the peak obtained for glassy carbon. Figure 11 compares the voltammograms for the two substrates onto which the Ni Mo deposit is formed by a clear nucleation mechanism. In figure 8 the voltammogram of Nianneal was also indicated in order to allow comparison between the three nickel substrates.

Deposits were performed by potentiostatic polarization at $-1200 \, mV$ for 3 h on the Nianneal and the 99.999% pure nickel. In both cases deposits were

Fig. 8. Voltammograms from Ni–Mo solution on various nickel electrodes: 99.9% Ni (····), 99.999% Ni (– – –), annealed 99.999% Ni (——). Scan rate $50 \, mV \, s^{-1}$.
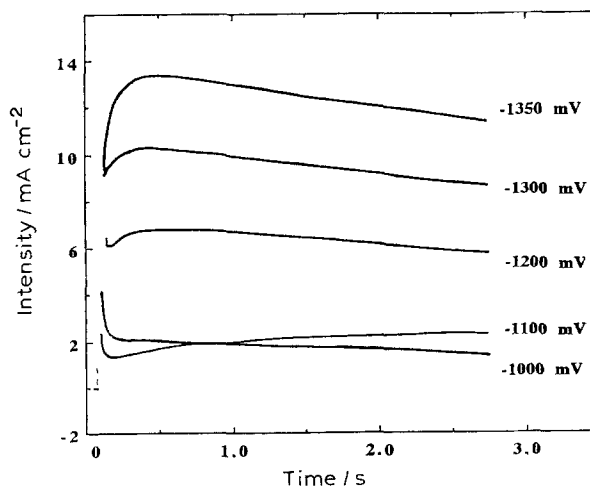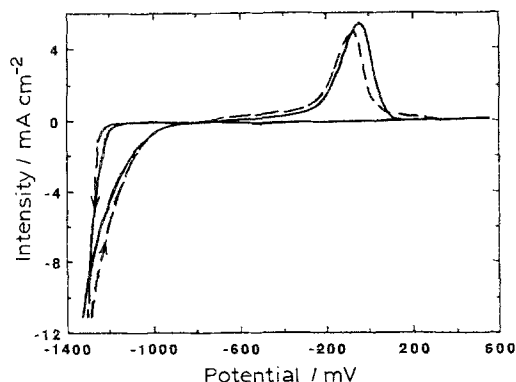

Fig. 10. Current–time transients from Ni–Mo solution on 99.9% Ni substrate.

Fig. 11. Voltammograms from Ni–Mo solution on: glassy carbon (- - -), and annealed 99.999% Ni (——). Scan rate 50 mV s⁻¹.

Fig. 13. Voltammograms from Ni–Mo solution on palladium. Scan rate 50 mV ⁻¹.

obtained, but that obtained on the annealed nickel was thicker, in keeping with the charge supplied. The influence of pH has been discussed in the work of Chassaing [5], and therefore two deposits were prepared from the Ni–Mo solution at pH 7 and 10 on Nianneal. The deposit obtained at pH 7 was bright and smooth but peeled off (Fig. 12). The deposit at pH 10 was nodular and adherent.

3.4. Palladium substrate

Figure 13 presents a voltammogram from a Ni–Mo solution on a palladium substrate. This trace does not correspond to the formation of a deposit by a nucleation mechanism. The current–time transient shows monotonic decrease in current. Although the formation of a deposit by epitaxial growth or precipitation seems unlikely, an experiment was performed to check whether a deposit can be formed under cath-
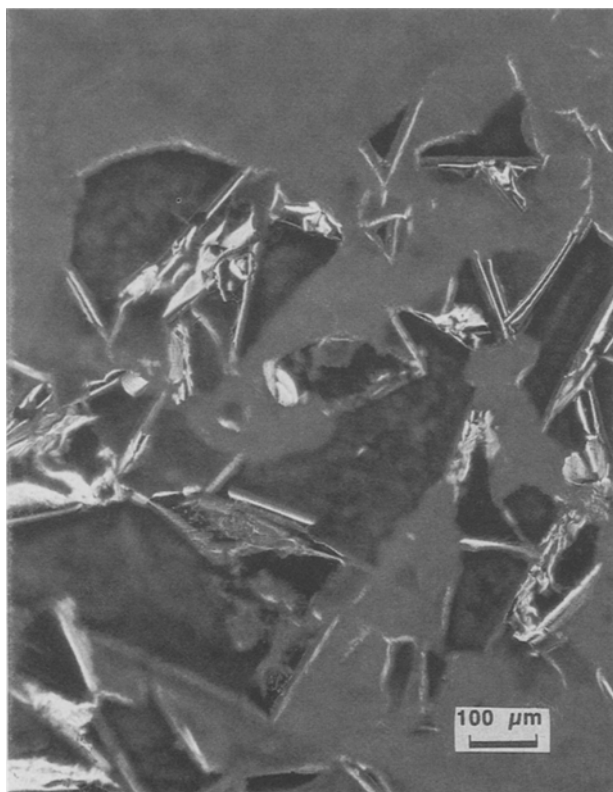

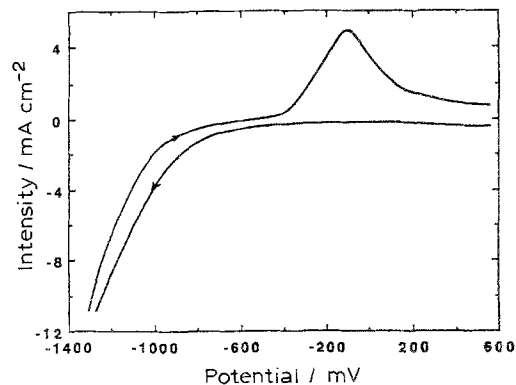Fig. 12. Deposit on nickel 99.999% (annealed).

odic polarization. The palladium was polarized at − 1200 mV for 2 h. Microscopic examination shows that the palladium has a brown colouring but no deposit is observed.

4. Discussion

4.1. Cathodic sweeps

Hydrogen evolution is completely different on two of the substrates used in this study: palladium substrate into which hydrogen diffusion is rapid and glassy carbon into which hydrogen does not diffuse. The voltammograms traced from the Ni–Mo solution indicate that on glassy carbon a deposit is formed by a nucleation mechanism, and that on palladium no nucleation occurs. The current-time transients obtained by cathodic potentiostatic polarization confirm the voltammograms. An attempt to prepare a bulk deposit on the two substrates in the same conditions succeeds in the case of glassy carbon, on which a thick deposit is obtained. In the case of palladium, only a brown colour is observed, indicating surface modification but no formation of a deposit.

By comparing the trace of hydrogen evolution on palladium recorded from citrate solution without Ni and Mo salts (Fig. 1) and from the Ni–Mo solution (Fig. 12), one can see that the overpotentials for hydrogen evolution are similar but the current intensity is about two times higher for the Ni–Mo solution, as if the hydrogen reaction were catalysed by the brown compounds formed on the palladium surface.

Some results [13] mention that nickel adsorbs electrolytically formed hydrogen, but the texture of the nickel used, i.e, its mechanical and heat treatment prior cathodic polarization, has never been evaluated. In this study, three specimens of nickel were used with various structural states of purity. The various results obtained with high purity nickel after and before annealing show the importance of grain size in hydrogen absorption. Small grains promote hydrogen diffusion, which is consistent with the thin deposit obtained on non-annealed nickel. Annealing, increases grain size and hence decreases hydrogen diffusion. Therefore the deposit obtained after heat treatment of the substrate is thicker. The behaviour of

an austenitic steel is similar, showing thicker Ni–Mo deposit after annealing of the substrate. Actually microstructural variations of the metal, as affected by heat treatment, can cause a wide range of hydrogen diffusion coefficients.

The cathodic part of the voltammograms, substantiated by the cathodic potentiostatic studies, shows the need for hydrogen, adsorbed on the electrode surface, to obtain metallic Ni–Mo alloys. The Ni–Mo alloys cannot be obtained on a substrate into which hydrogen diffusion occurs.

4.2. Anodic sweeps

The general feature of the voltammograms is the presence of one or two anodic peaks, except in the case of the carbon substrate, even when there is no reducible metallic salt in the citrate solution.

Coming back to the palladium electrode in citrate solution, the two anodic peaks might be explained by the dissolution of the substrate, but the inertness of this metal in most of the solutions is inconsistent with such an anodic peak. Moreover, when the anodic scan started from the equilibrium potential of hydrogen, there was no anodic peak. As hydrogen diffuses rapidly into palladium, the two anodic peaks must correspond to the oxidation of hydrogen [13]. Following the study of Chao et al. [9], these two peaks can be attributed to absorbed and adsorbed hydrogen. When the Ni–Mo solution was used, on palladium substrate, only one peak existed and its potential corresponded to the second anodic peak observed in citrate solution. The charge passed under the anodic peak from the Ni–Mo solution is more than three times that from citrate solution without plating salts, showing the catalytic effect of the molybdenum species on hydrogen evolution.

On the other hand, for glassy carbon there is no significant current within the potential anodic region when the voltammogram is traced from citrate solution, but the voltammogram recorded from the Ni–Mo solution presents one anodic peak at the same potential as that obtained for palladium. In this case a deposit is formed on the carbon and this peak could be explained by the Ni–Mo alloy dissolution. But Ni–Mo alloys are of the Hastelloy type, whose corrosion resistance is well known. Some polarization curves performed with bulk Hastelloy indicate the inertness of this alloy. This result is confirmed by immersion corrosion test performed on a Ni–Mo alloy deposited on steel [8], which have shown that the Ni–Mo alloy is corrosion resistant but, because of the porosity of the deposit, the solution can reach the substrate and attack it. In the present study, as the substrate is glassy carbon, there is no possibility for the peak to correspond to the dissolution of the substrate, and this peak also indicates hydrogen oxidation. Glassy carbon cannot absorb hydrogen, and therefore this oxidized hydrogen comes from the alloy deposit, in which it is trapped during the
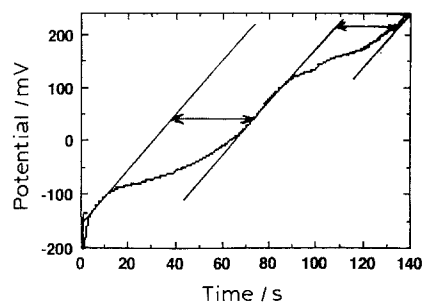

Fig. 14. Galvanostatic oxidation of hydrogen, after charging at cathodic potential ($-1200\,$mV). $i = 5\,$mA cm^{-2}. On 99.999% Ni substrate.

expanding of the lattice by codeposition of metal and hydrogen.

For the annealled high purity nickel, the voltammogram is similar to that for carbon and, particularly, the anodic peak is identical (Fig. 11) and corresponds to the oxydation of hydrogen trapped in the deposit. To show the presence of hydrogen in the NiMo alloy, a bulk deposit was performed by cathodic polarization at a constant potential of $-1200\,$mV for 20 min. Owing to the codeposition of metal and hydrogen, hydrogen absorption is easy because it is trapped in the growing deposit. The desorption of hydrogen was carried out at constant anodic current. As hydrogen tends to form molecular hydrogen spontaneously, the oxidized hydrogen will be less than the actual quantity. The potential-time transient in Figure 14 shows two transition times. Such a galvanostatic transient was obtained by Chao et al. [9] for the oxidation of hydrogen after charging a gold cathode, and the transitions were attributed to weakly and strongly bonded hydrogen. In the case of Ni–Mo the deposit, which traps hydrogen in its lattice, is formed on a substrate which is also able to retain hydrogen. Hence, in a first approach, the first transition time is attributed to hydrogen trapped in the deposit, and the second one to the hydrogen from the nickel. The same experiment performed with glassy carbon substrate exhibits only one transition time, the carbon being unable to retain hydrogen. Further experiments are planned to substantiate this hypothesis.

5. Conclusion

This study has confirmed the need for hydrogen to obtain the formation of a Ni–Mo alloy deposit. On glassy carbon, where there is no possiblity for hydrogen to diffuse into the substrate, the deposit is thick, crystallized or amorphous depending on the pH of the solution. If the substrate, as for instance palladium, absorbs hydrogen, the deposit cannot be obtained. If the substrates do not have such an extreme behaviour towards hydrogen, as for example nickel or steel, the structure of the metal plays an important part. A great quantity of hydrogen is trapped in the Ni–Mo alloy by codeposition with the metals.

la Recherche et de la Technologie, France) Contract no. 89A0017.

References

[1] E. Beltoska-Lehman, *J. Appl. Electrochem.* **20** (1990) 132.
[2] I. Arul Raji and K. I. Vasu, *ibid.* **20** (1990) 32.
[3] D. E. Brown, M. N. Mahmood, M. C. M. Man and K. Turner, *Electrochim. Acta* **29** (1984) 1551.
[4] C. M. Lacnjevac, N. M. Markovic and M. M. Jaksic, *Surf. Technol.* **22** (1984) 51.
[5] E. Chassaing, Thèse doctorat-ès-sciences, Paris VI (1975).
[6] C. C. Nee, W. Kim and R. Weil, *J. Electrochem. Soc.* **135** (1988) 1100.
[7] E. Chassaing and K. Vu Quang, *J. Appl. Electrochem.* **19** (1989) 839.
[8] M. Degrez and R. Winand, *Oberfläche Surface* **8** (1990) 8.
[9] F. Chao and M. Costa, Second International Congress on Hydrogen in Metals, Paris (1977).
[10] R. Le Penven, W. Levason and D. Pletcher, *J. Appl. Electrochem.* **20** (1990) 399.
[11] D. D. MacDonald, Transients techniques in Electrochemistry, Plenum Press, New York (1977).
[12] G. D. Wilcox, D. R. Gabe and M. E. Warwick, *Corros. Sci.* **28** (1988) 577.
[13] H. E. G. Rommal and P. J. Morgan, *J. Electrochem. Soc.* **132** (1988) 343.